Electronic Supplementary Material (ESI) for Nanoscale.

Electronic Supplementary Information

Theoretical insights into a potential lead-free hybrid perovskite: substituting Pb^{2+} with Ge^{2+}

Ping-Ping Sun, Quan-Song Li,* Li-Na Yang, Ze-Sheng Li *

Key Laboratory of Cluster Science of Ministry of Education, Beijing Key Laboratory of Photoelectronic/Electrophotonic Conversion Materials, School of Chemistry, Beijing Institute of Technology, Beijing 100081, China

* Corresponding author at: 5 South Zhongguancun Street Haidian Zone, Beijing 10081, China. Tel.: +86 10 68918670; fax: +86 10 68918670

E-mail: liquansong@bit.edu.cn; zeshengli@bit.edu.cn.

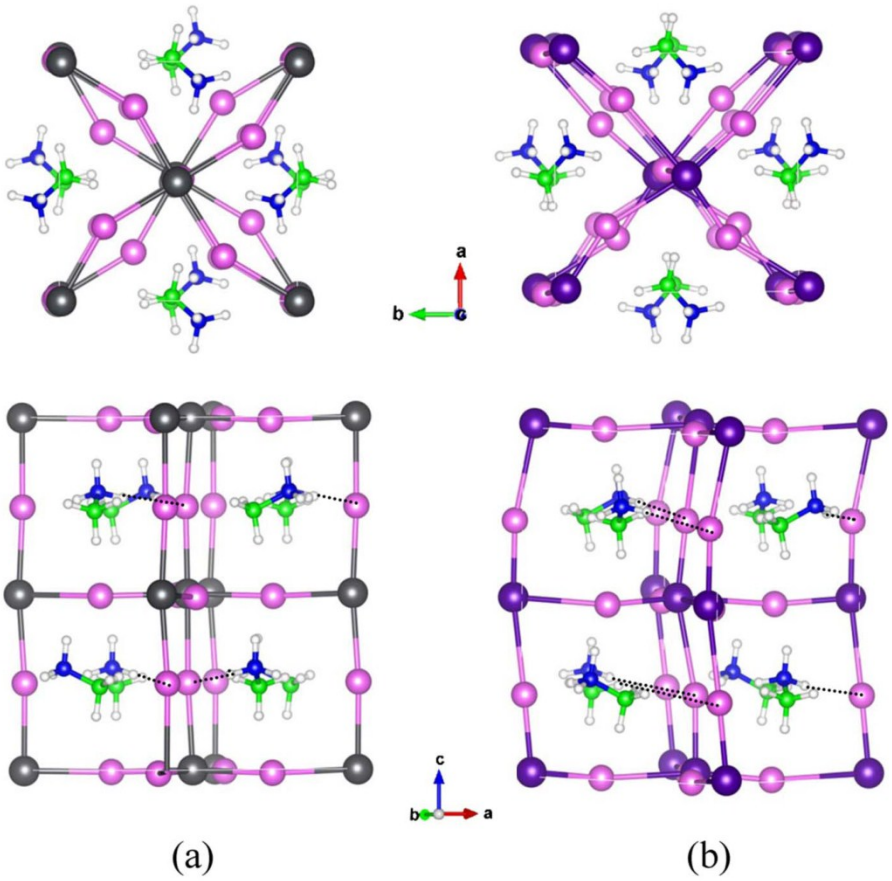

Fig. S1 Optimized stable geometries of (a) $MAPbI_3$, (b) $MASnI_3$. The upper panel is top view, the under panel is side view. (brown: Pb; plum: Sn; pink: I; green: C; blue: N; white: H)

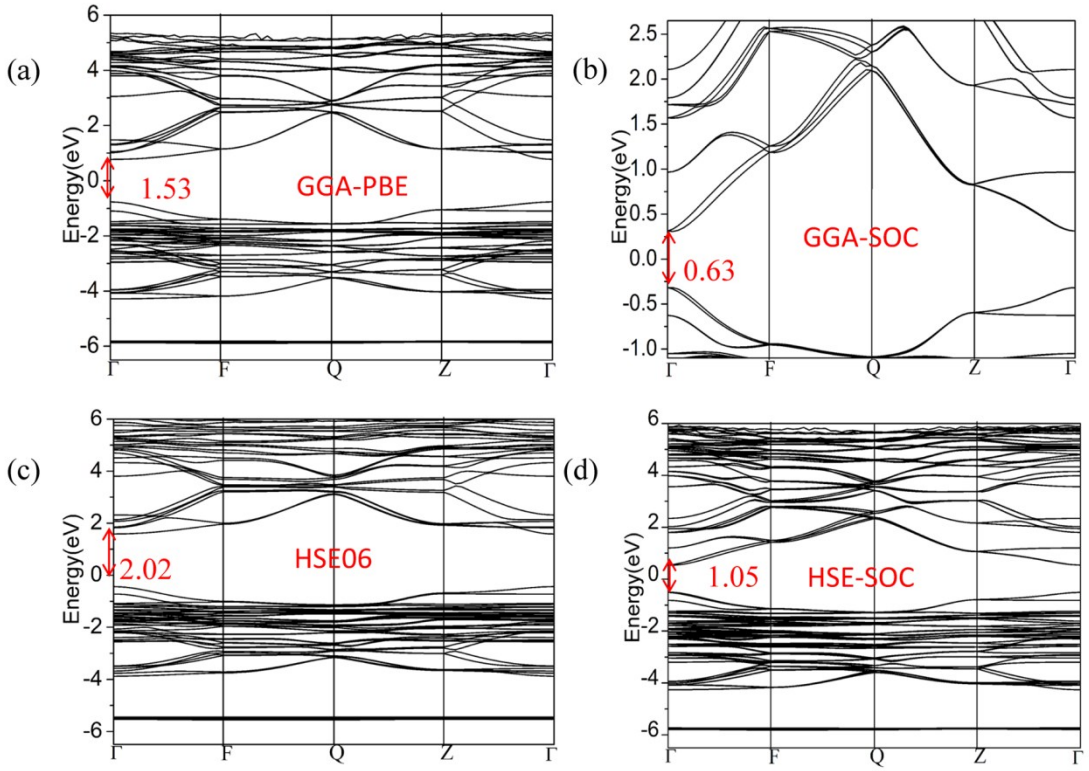

Fig. S2 Band structures of $MAPbI_3$ with (a) GGA-PBE, (b) PBE-SOC, (c) HSE06 and (d) HSE-SOC methods. Since the experimental band gap of $MAPbI_3$ is in the range of 1.5-1.66 eV, the PBE result matches well with its experimental data. PBE-SOC result shows 1 eV less than that of the GGA-PBE on account of the SOC energy splitting effect. A more accurate calculation hybrid functional HSE06 used for this structure shows a little higher value than its experimental data, which can be interpreted as the Coulomb potential effect for heavy elements that stretches the conduction bands energies. The HSE-SOC result shows a reduction to its experimental data, it may due to the big SOC effect of Pb which pulls down the conduction band.

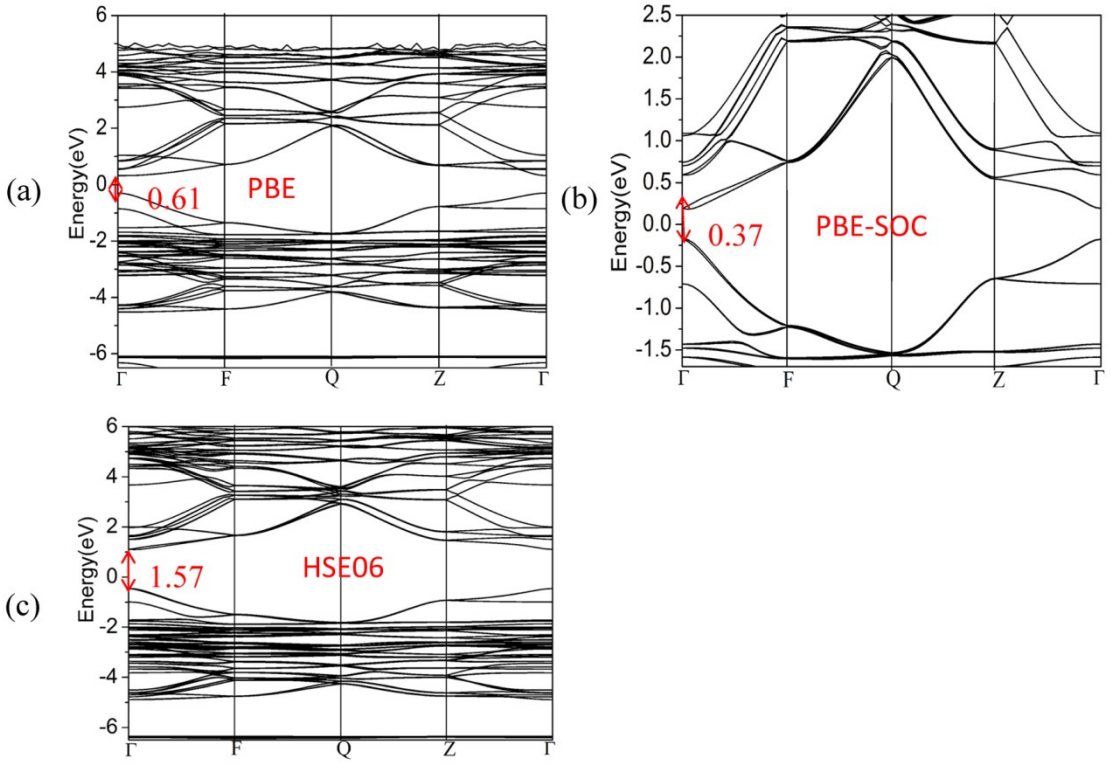

Fig. S3 Band structures of $MASnI_3$ with (a) GGA-PBE, (b) PBE-SOC, (c) HSE06 methods. The PBE result underestimates the band gap of $MASnI_3$ by 0.6 eV, while PBE-SOC calcultaion gives almost 1 quarter of its experimental value since SOC shows a great impact on Sn and I elements, which lowers the band gap by splitting its conduction band energy. For hybrid HSE06 calcution, it gives nearly 0.4 eV wider band gap than its experimental value.

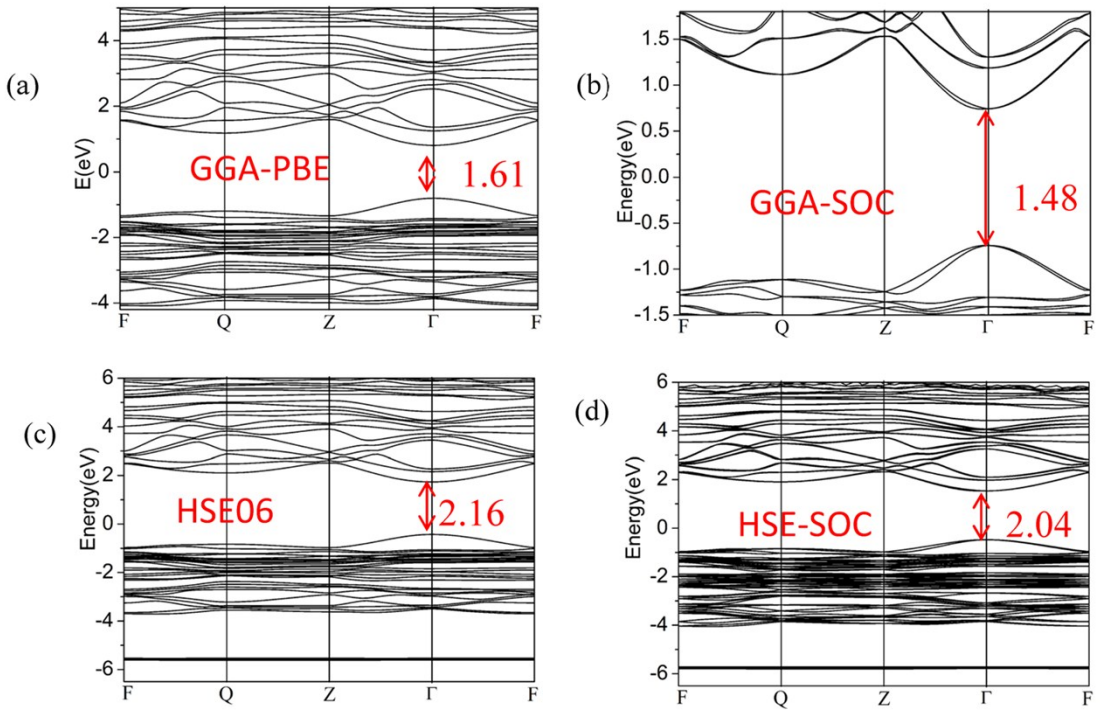

Fig. S4 Band structures of $MAGeI_3$ with (a) GGA-PBE, (b) PBE-SOC, (c) HSE06 and (d) HSE-SOC methods. The PBE result of $MAGeI_3$ is similar to that of $MAPbI_3$ (1.534 eV). It seems that for both $MAGeI_3$ and $MAPbI_3$ perovskites, the GGA-PBE method is enough to describe the precision of the calculation. For PBE-SOC method, its result is only 0.126 eV lower than its PBE value, which indicates that the SOC effect on $MAGeI_3$ is weaker than that of $MAPbI_3$ and $MASnI_3$. As to hybrid functional calculation, HSE06 with a 2.112 eV value is higher than that of $MAPbI_3$ (2.024 eV). Up to now, the HSE06 results of the three mentioned systems are all higher than their corresponding experimental value although it can give the detailed band energy oscillation along the symmetric K points in the Brillouin-zone. The band gap with HSE-SOC agrees well with its experimental result (1.9 eV), since the combination of HSE06 and SOC can give an accurate result by push-pull energy counteract.

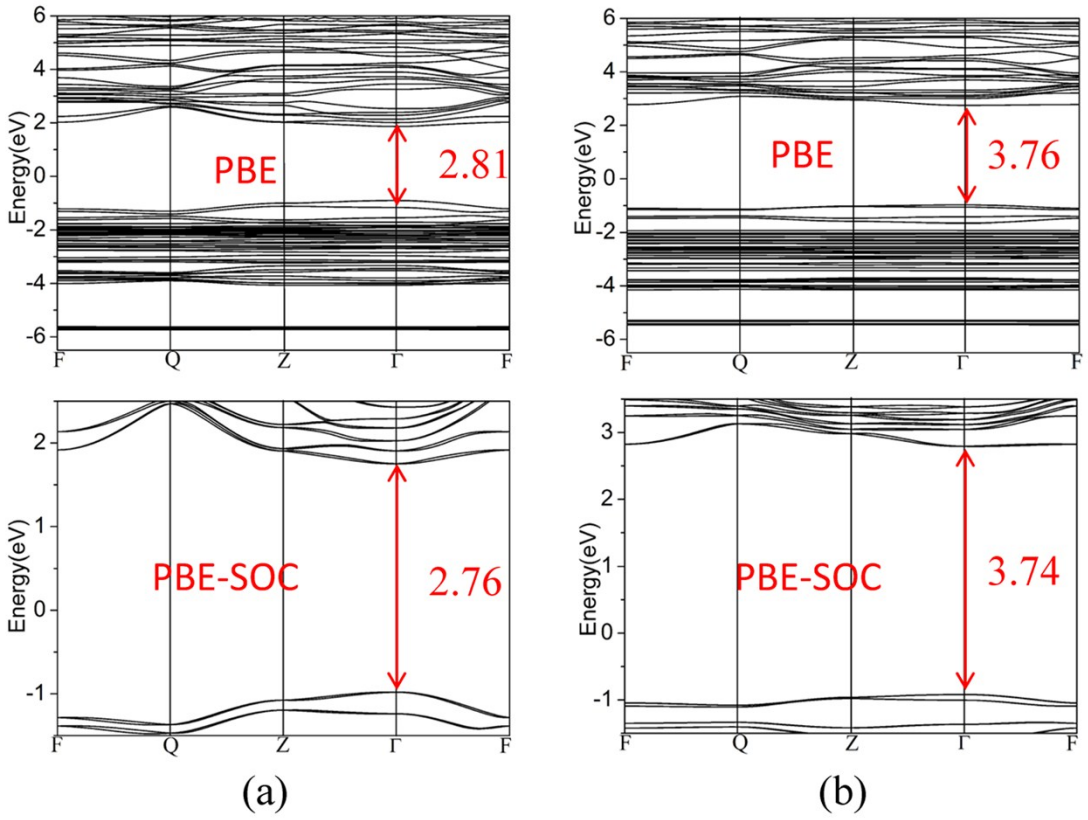

Fig. S5 Band structures of (a) $MAGeBr_3$, (b) $MAGeCl_3$ with GGA-PBE and PBE-SOC methods. Both the two calculation methods for Br- and Cl-based perovskites give wide band gaps, since the materials with wide band gap are unsuitable for the perovskite application, so HSE06 and HSE-SOC calculations are not adopted for the two systems. On account of the band gap compatibility with $MAPbI_3$, $MAGeI_3$ can act as a new candidate of the three Ge-based perovskites to substitute the potential pollutant Pb-based perovskites.

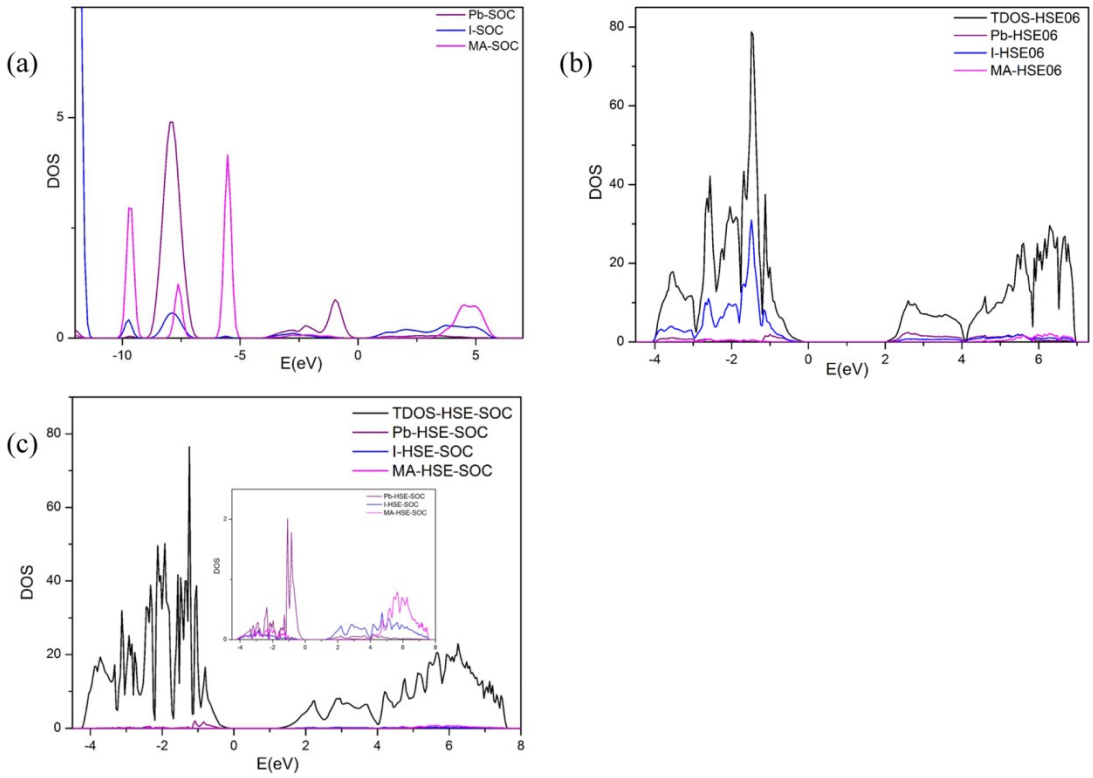

Fig. S6 DOS structures of $MAPbI_3$ with (a) PBE-SOC, (b) HSE06 and (c) HSE06-SOC methods. The orbital contributions of conduction bands and valence bands show a similarity among the three calculation methods. PDOS of both PBE-SOC and HSE-SOC give weak peak intensity as shown in (a) and (c) with the peak heights no more than 5, which are almost one fifth of the peak intensities of HSE06 results. This weak peak intensity can be interpreted as the energy splitting effect caused by SOC, which weakens the peak intensities of heavy elements. The DOS and PDOS of the two hybrid functionals HSE06 and HSE-SOC show more acute and intensive volatility, which give detailed orbital contribution changed with the corresponding band energy oscillation.

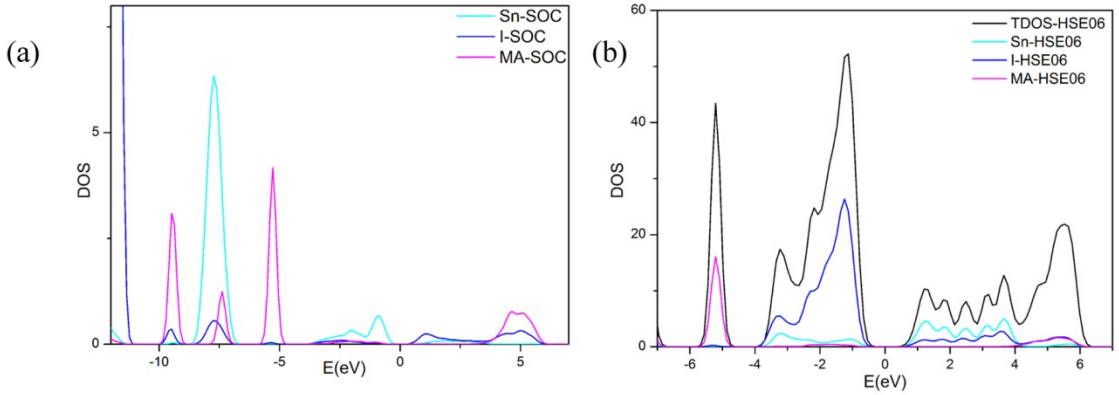

Fig. S7 DOS structures of $MASnI_3$ with (a) PBE-SOC, (b) HSE06 methods. As same as $MAPbI_3$, PDOS of $MASnI_3$ also give weak contribution under the SOC effect, for Sn and I are shown with large spin-orbit coupling constant. Although the DOS and PDOS under the two calculation methods demonstrate a similarity in peak shape, the peak strengthes with PBE-SOC show great weaker than those of HSE06.

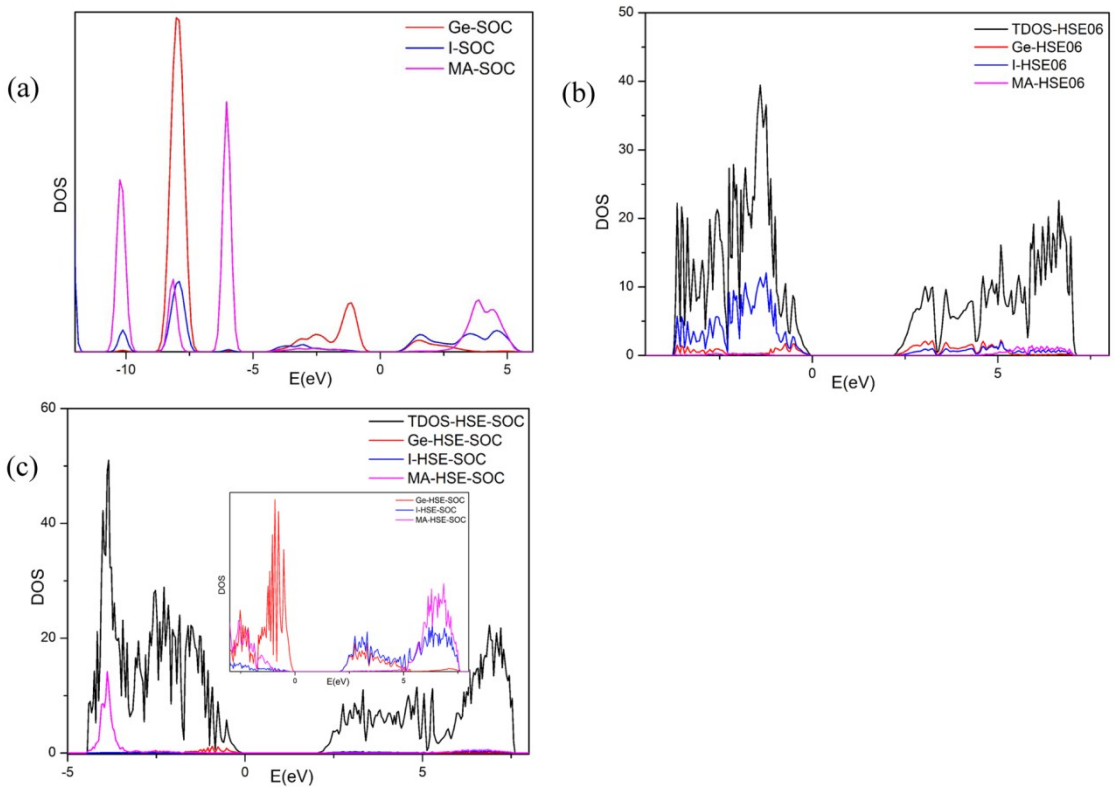

Fig. S8 DOS structures of $MAGeI_3$ with (a) PBE-SOC, (b) HSE06 and (c) HSE06-SOC methods. According to the comparability between $MAGeI_3$ and $MAPbI_3$ in band gap as mentioned above, the DOS and PDOS of the two systems also show the similarity both in peak shape and peak intensity under the same conditions, which also confirms that $MAGeI_3$ can demonstrate the good electronic character as that of $MAPbI_3$.

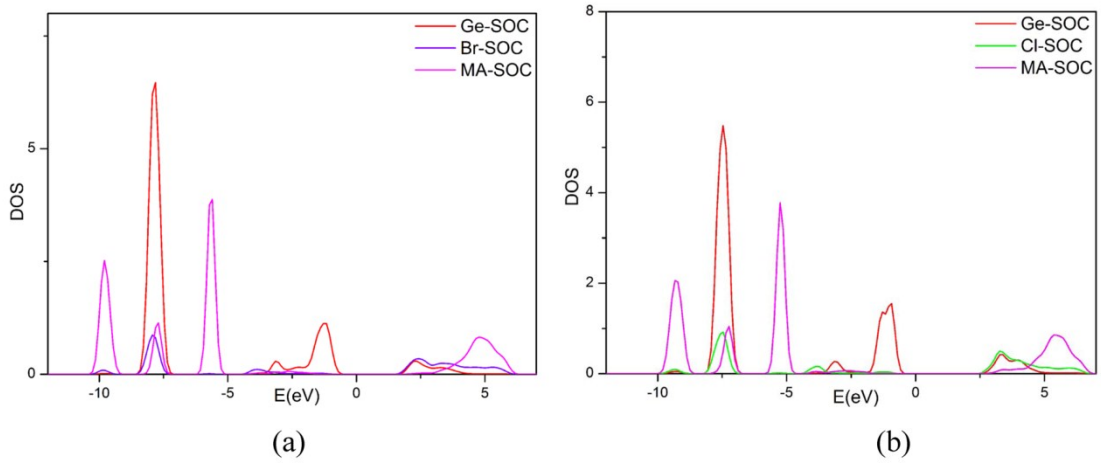

Fig. S9 DOS structures of $MAGeBr_3$ and $MAGeCl_3$ with PBE-SOC method. The main contribution of this material is composed of s orbial of Ge and p orbitals of Br/Cl for valence bands and p orbitals of Ge and Br/Cl for conduction bands.

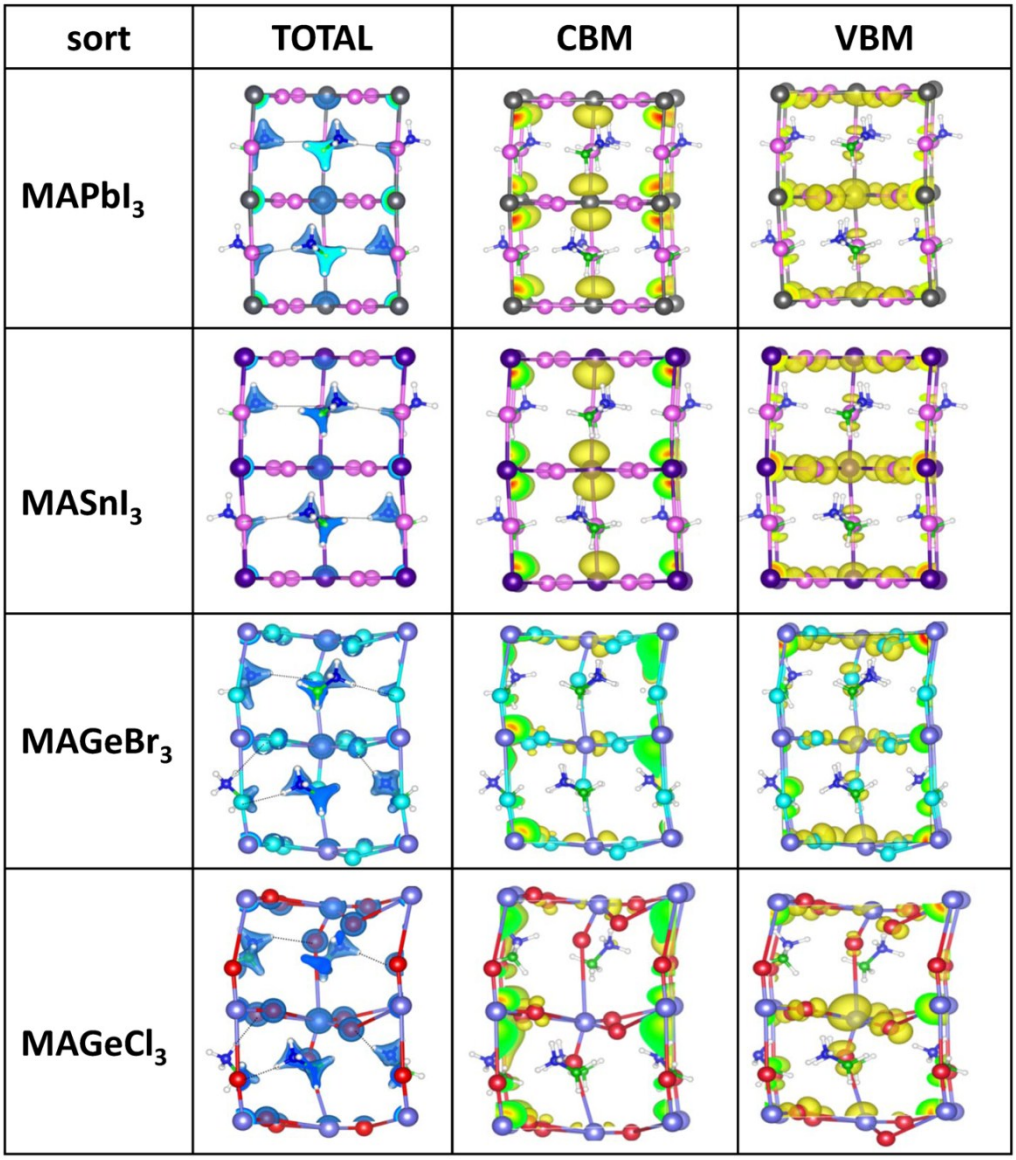

Fig. S10 Charge density of $MAPbI_3$, $MASnI_3$, $MAGeBr_3$ and $MAGeCl_3$. The left panel is total charge density, the middle panel is CBM charge density, the right panel is VBM charge density. For CBM, the electrons are accumulated at metal (Pb and Sn), while for VBM, holes are distributed around metal and halogens, which show the same contribution as we can get from their DOS structures. The separation of electrons and holes between CBM and VBM will promote the electron excitation.

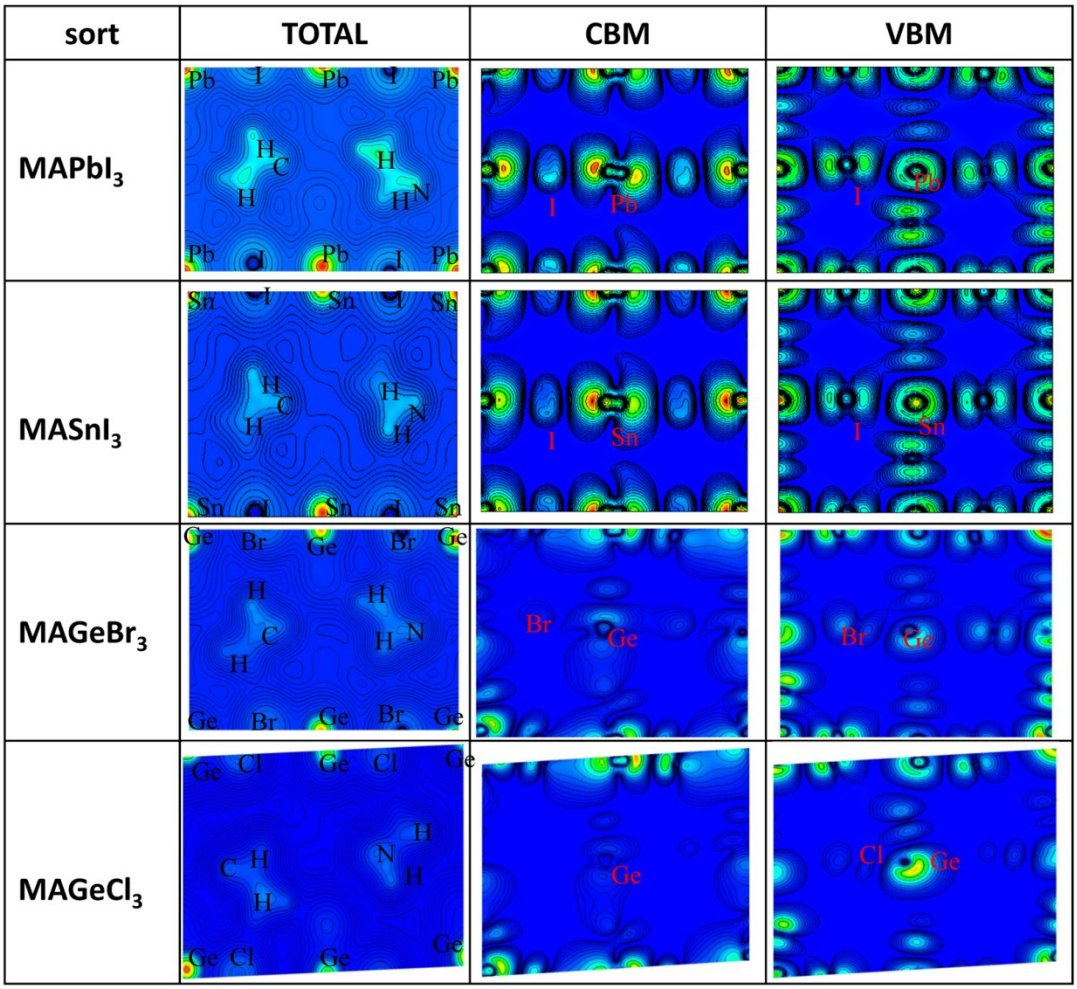

Fig. S11 Electrostatic potential of $MAPbI_3$, $MASnI_3$, $MAGeBr_3$ and $MAGeCl_3$. The left panel is total electrostatic potential of (100) surface, the middle panel is CBM electrostatic potential of (110) surface, the right panel is VBM electrostatic potential of (110) surface.

Table S1 Effective mass m* and the corresponding reduced masses μ for the researched systems in F-Q, Q-Z, Z-Γ directions for $MAPbI_3$, $MASnI_3$ and $MAGeI_3$.

	$MAPbI_3$			$MASnI_3$			$MAGeI_3$		
	m_e	m_h	μ	m_e	m_h	μ	m_e	m_h	μ
				PBE					
F-Q	0.253	0.453	0.162	0.263	0.239	0.125	0.244	0.247	0.123
Q-Z	0.213	0.339	0.131	0.205	0.181	0.096	0.209	0.242	0.112
Z-Γ	0.120	0.268	0.083	0.225	0.221	0.111	0.195	0.231	0.106
				PBE-SOC					
F-Q	0.217	0.319	0.129	0.258	0.235	0.123	0.221	0.223	0.111
Q-Z	0.204	0.335	0.127	0.193	0.171	0.091	0.196	0.213	0.102
Z-Γ	0.115	0.212	0.074	0.221	0.212	0.108	0.172	0.175	0.087
				HSE06					
F-Q	0.201	0.308	0.122	0.214	0.196	0.105	0.211	0.216	0.104
Q-Z	0.188	0.278	0.112	0.187	0.169	0.089	0.173	0.186	0.089
Z-Γ	0.104	0.197	0.068	0.198	0.183	0.095	0.146	0.167	0.077
				HSE-SOC					
F-Q	0.109	0.236	0.075	-	-	-	0.141	0.142	0.071
Q-Z	0.102	0.221	0.070	-	-	-	0.138	0.159	0.074
Z-Γ	0.095	0.154	0.059	-	-	-	0.129	0.148	0.069

Table S2 Effective mass m* and the corresponding reduced masses μ for the researched systems in F-Q, Q-Z, Z-Γ directions for $MAGeBr_3$ and $MAGeCl_3$.

	$MAGeBr_3$			$MAGeCl_3$		
	m_e	m_h	μ	m_e	m_h	μ
			PBE			
F-Q	0.581	0.338	0.214	0.311	0.318	0.157
Q-Z	0.491	0.233	0.158	0.326	0.304	0.157
Z-Γ	0.398	0.396	0.198	0.312	0.341	0.163
			PBE-SOC			
F-Q	0.431	0.325	0.185	0.272	0.231	0.125
Q-Z	0.323	0.208	0.131	0.248	0.214	0.115
Z-Γ	0.314	0.282	0.148	0.219	0.285	0.124